

Calculation of Frequency-Dependent Impedance for Conductors of Rectangular Cross Section

Alexander W. Barr
AMP Incorporated

ABSTRACT

Knowledge of the resistance and self-inductance of a contact as well as the mutual inductance between contacts is often necessary in determining the high-speed performance of connectors. Many of these connectors contain pins with rectangular cross sections. Such geometries cannot be easily handled through analytical techniques. This paper presents a numerical technique where the conductor cross sections are broken into subconductors and the frequency-dependent current amplitude in each subconductor is found by solving a system of equations relating the resistances, self-inductances, and mutual inductances of all the subconductors. Once the currents in the subconductors are known, they are used to compute the frequency-dependent resistance and self-inductance of an individual conductor and the effective resistance and inductance of a conductor pair. Also the currents of the subconductors are graphed to give a discretized representation of the current density in the conductors.

INTRODUCTION

Spiraling advances in electronic technology are placing an ever increasing burden on connector manufacturers. With computer clock frequencies doubling every few years and

semiconductor manufacturers fabricating chips requiring hundreds of interconnects, systems packaging becomes critical. Customers want to produce densely packaged systems to carry high-speed signals at low cost.

Several electrical challenges are presented by this desire. First, high-speed signals usually contain pulses with fast rising and falling edges. Critical to the production of these fast transitions is the high-frequency content of the pulse. Unfortunately, risetime degradation often occurs because these high-frequency components are easily attenuated. Impedance-matched interconnections can be used to minimize the possibility of compromising these edge rates.

Second, the significant voltage gradients attendant with fast risetimes couple effectively with neighboring lines in the form of crosstalk. Crosstalk can cause distortion of the original signal and possibly lead to false triggering of the connected circuitry. Dense packaging only tends to exacerbate this problem. System designs need to be reviewed in terms of their prospective susceptibility to crosstalk problems.

Third, high-speed signals travel short distances between voltage transitions. If interconnections are long, or of dissimilar lengths, propagation delays can affect signal synchronization and system integrity. Propagation delays need

to be minimized and signal path lengths should be consistent.

To assess the impact of interconnections on these signal integrity issues, it is necessary to compute the frequency-dependent impedance of the interconnects. In the case of circular-shaped wires or pins, this task can be accomplished through analytical techniques. However, many connectors contain pins or contacts of rectangular cross section. The behavior of such conductors can only be accurately examined through use of numerical methods.

This paper describes a numerical technique for computing the frequency-dependent resistance and inductance of conductors with rectangular cross sections. The cases of both a single isolated conductor and two conductors experiencing mutual coupling are addressed: The conductors are divided into subconductors and the frequency-dependent current amplitude in each subconductor is found by solving a system of equations relating the resistances and self-inductances of, and mutual inductances between, the subconductors. Once the currents in the subconductors are known, they are used to compute the frequency-dependent resistance and self-inductance of each conductor and the effective resistance and inductance of a conductor pair. Furthermore, the current amplitudes of the subconductors can be graphed to give a discretized visual representation of the current density in the conductors.

FREQUENCY-DEPENDENT IMPEDANCE FOR A SINGLE CONDUCTOR

Before computing the impedance of an individual conductor of rectangular cross section, it is instructive to understand the motivation behind pursuing the announced technique. It is well known that at dc, the current in a conductor is evenly distributed across the cross section. As frequency increases the current tends to crowd toward the outside of the conductor, until at high frequencies it is almost completely confined to a thin skin near the surface. If the conductor's cross section is subdivided into much smaller sections, the current density in each subconductor will be almost uniform across the subconductor's cross section. By assuming that these subconductor current densities are indeed uniform, the subconductors can be treated as circuit components. Once a circuit model representation of the original conductor has been constructed from these components, the subconductor currents can be computed and the impedance of the conductor can be found.

Figure 1 shows a rectangular post of width W , thickness T , and length ℓ , being driven by a sinusoidal generator operating at angular frequency $\omega = 2\pi f$. If this post is divided into N_w subconductors across the width and N_t subconductors across the thickness, there will be $N = N_w N_t$ total subconductors. Each of these subconductors will have a width, $w = W/N_w$, and a thickness, $t = T/N_t$.

To find the resistance and self-inductance for this post at the frequency of interest, the resistance and inductance for the

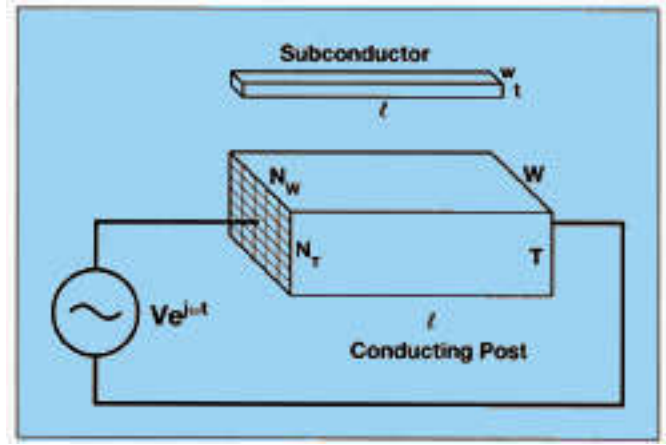


Figure 1. Single conducting post driven by a sinusoidal generator.

individual subconductors must first be computed. If the conductivity \mathbf{s} for the post is known, then the resistance of a subconductor will be

$$R = \frac{\ell}{\sigma w t} \quad (1)$$

If ℓ is large compared to w and t (at least five times greater), Keiser¹ has shown that the self-inductance, L , for the subconductors will be

$$L = 0.2 \ell \left[\ln \left(\frac{2\ell}{w+t} \right) + 0.5 + 0.2235 \frac{w+t}{\ell} \right] \mu H, \quad (2)$$

if ℓ , w , and t are in meters. Similarly, Grover² has shown that the mutual inductance between two posts is ostensibly the same as between two filaments located at the posts' centers. Therefore, the mutual inductance between the subconductor in the i^{th} row and j^{th} column and the subconductor in the m^{th} row and n^{th} column will be

$$M_{ij, mn} = 0.2 \ell \left[\ln \left(\frac{\ell}{d_{ij, mn}} + \sqrt{1 + \frac{\ell^2}{d_{ij, mn}^2}} \right) - \sqrt{1 + \frac{d_{ij, mn}^2}{\ell^2} + \frac{d_{ij, mn}}{\ell}} \right] \mu H, \quad (3)$$

where $d_{ij, mn}$ is the distance between the center axes of the subconductors, ℓ is the length of both subconductors, and $d_{ij, mn}$ and ℓ are in meters. Note that this formula exhibits some inaccuracy when the subconductors are close together (distances on the order of the cross-sectional dimensions). However, it has been found that the minor errors this equation sometimes introduces have an insignificant impact on the frequency-dependent impedance computation.

Once calculations have been completed to find the resistance and self-inductance of the subconductors as well as the mutual inductances between all the subconductors, a system of equations can be constructed to determine the subconductor currents.

The laws of electromagnetism dictate that the voltage drop across the length of a conductor is the same regardless of where, in the conductor cross section, the current travels.

Therefore, if the voltage drop across the post is V , the drop across each of the subconductors is also V . Ohm's law says that the voltage drop will be equal to the impedance multiplied by the current. In this case, the impedance is a combination of the resistance and self-inductance of the given subconductor as well as the mutual inductance between the chosen subconductor and each of the other subconductors. For the subconductor in the i^{th} row and j^{th} column, this voltage will be

$$\begin{aligned}
 V = & I_{11} j\omega M_{11,j} + I_{12} j\omega M_{12,j} + \dots + I_{1N_w} j\omega M_{1N_w,j} + \\
 & I_{21} j\omega M_{21,j} + I_{22} j\omega M_{22,j} + \dots + I_{2N_w} j\omega M_{2N_w,j} + \\
 & I_{i1} j\omega M_{i1,j} + \dots + I_{ij} (R + j\omega L) + \dots + I_{iN_w} j\omega M_{iN_w,j} + \\
 & I_{N_11} j\omega M_{N_11,j} + I_{N_12} j\omega M_{N_12,j} + \dots + I_{N_1N_w} j\omega M_{N_1N_w,j} + \dots
 \end{aligned} \tag{4}$$

where $\mathbf{v} = 2\pi f$. A similar expression can be developed for each of the subconductors, creating a system of N equations in N unknowns where the unknowns are the subconductor currents:

$$\begin{bmatrix} V \\ V \\ \vdots \\ V \\ V \end{bmatrix} = \begin{bmatrix} R + j\omega L & j\omega M_{12,11} & \dots & j\omega M_{N_1N_w,11} \\ j\omega M_{11,12} & R + j\omega L & \dots & j\omega M_{N_1N_w,12} \\ \vdots & \vdots & \ddots & \vdots \\ j\omega M_{11,i1} & j\omega M_{12,i1} & \dots & j\omega M_{N_1N_w,i1} \\ j\omega M_{11,N_1N_w} & j\omega M_{12,N_1N_w} & \dots & R + j\omega L \end{bmatrix} \begin{bmatrix} I_{11} \\ I_{12} \\ \vdots \\ I_{ij} \\ I_{N_1N_w} \end{bmatrix} \tag{5}$$

This equation is just a matrix expression of Ohm's law. Since the voltage vector V and the elements of the impedance matrix are already known, the system can be solved for the current vector.

Solving this matrix involves finding the inverse of the impedance matrix and premultiplying it by the voltage vector. Numerous ways exist to find the inverse of square matrices. However, matrix size, conditioning of the elements, desired accuracy, and required speed of solution all influence the choice of an algorithm. Because of its efficiency and resilience to roundoff errors, LU Decomposition was used to invert the impedance matrix. This method involves decomposing the impedance matrix into the product of a lower triangular matrix and an upper triangular matrix. Substitution can be easily used to solve the resulting two systems of equations and find the inverse of the original matrix. More discussion of this method can be found in the references.

Once the current vector is known, the currents in each of the subconductors have been determined. Since these sub-currents all flow in parallel, the total current through the post is

$$I = \sum_{i=1}^{N_T} \sum_{j=1}^{N_w} I_{ij} \tag{6}$$

Consequently, the impedance of the whole post is

$$\frac{V}{I} = Z = R_{\text{post}} + j\omega L_{\text{post}} \tag{7}$$

where R_{post} and L_{post} are the resistance and self-inductance of the post at the frequency f .

To illustrate the development of the skin effect with rising frequency, the subconductor currents can be plotted relative to their position in the post to give a discrete approximation to the cross-sectional current density. Such plots are shown later in this paper.

FREQUENCY DEPENDENT IMPEDANCE FOR TWO CONDUCTORS CARRYING EQUAL CURRENTS

Two posts, each carrying current I , and connected in series to a generator oscillating at frequency f , are illustrated in Figure 2. Post 1 is T_1 thick, W_1 wide, and ℓ long. Post 2 is T_2 thick, W_2 wide, and ℓ long. If the posts are divided into N_{1w} and N_{2w} subconductors across their widths and N_{1t} and N_{2t} subconductors across their thicknesses, the total number of subconductors in each will be $N_1 = N_{1t}N_{1w}$ and $N_2 = N_{2t}N_{2w}$, for post 1 and post 2, respectively. The widths and thicknesses for the subconductors in each post will be

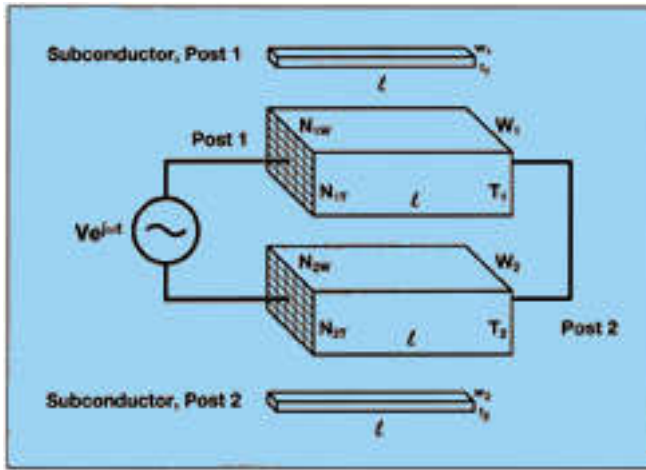


Figure 2. Two conducting posts in series driven by a sinusoidal generator.

$$w_1 = \frac{W_1}{N_{1W}}, \quad t_1 = \frac{T_1}{N_{1T}}, \quad w_2 = \frac{W_2}{N_{2W}}, \quad t_2 = \frac{T_2}{N_{2T}}. \quad (8)$$

As in the calculation for the single post, equations (1) and (2) are used to compute the resistance and self-inductance of each subconductor. Equation (3) also yields the mutual

inductance between subconductors. However, care must be taken to consider the directions of the currents in the two subconductors. If the currents are in the same direction, the mutual inductance will be positive; if the currents are in opposite directions, the mutual inductance will be negative. Consequently, the mutual inductances between subconductors in the same post will always be positive; mutual inductances between subconductors in different posts will be positive or negative depending on the direction of current.

Once the resistance and inductance values were determined for the various subconductors in the single post, equation (4) was constructed expressing the voltage drop across a given subconductor. A somewhat different approach is taken this time. It was initially assumed that the posts were connected in series so that the currents would be the same in each. Because the voltage V of the generator is dropped across the two posts together, any voltage drop equations that are constructed must include the drop across a subconductor in post 1 and a subconductor in post 2. It is only by choosing these pairs of subconductors—one from each post—that equations relating to the generator voltage V can be constructed. Consequently, a subscripting system is adopted using three integers. The first subscript designates the post, the second designates the row of the subconductor, and the third designates the column of the subconductor. Using this system, the voltage drop across the subconductor in the i^{th} row and j^{th} column of post 1 and the subconductor in the m^{th} row and n^{th} column of post 2 has the form:

$$\begin{aligned} V_{1ij} = & I_{111} j\omega M_{111,1ij} + I_{112} j\omega M_{112,1ij} + \dots + I_{1N_{1W}} j\omega M_{11N_{1W},1ij} + \dots + \\ & I_{111} j\omega M_{111,1ij} + \dots + I_{1ij} (R_1 + j\omega L_1) + \dots + I_{1N_{1W}} j\omega M_{11N_{1W},1ij} + \dots + \\ & I_{1N_{1T}1} j\omega M_{11N_{1T}1,1ij} + I_{1N_{1T}2} j\omega M_{11N_{1T}2,1ij} + \dots + I_{1N_{1T}N_{1W}} j\omega M_{11N_{1T}N_{1W},1ij} - \\ & I_{211} j\omega M_{211,1ij} - I_{212} j\omega M_{212,1ij} - \dots - I_{21N_{2W}} j\omega M_{21N_{2W},1ij} - \dots - \\ & I_{2m1} j\omega M_{2m1,1ij} - \dots - I_{2mn} j\omega M_{2mn,1ij} - \dots - I_{2mN_{2W}} j\omega M_{2mN_{2W},1ij} - \dots - \\ & I_{2N_{2T}1} j\omega M_{2N_{2T}1,1ij} - I_{2N_{2T}2} j\omega M_{2N_{2T}2,1ij} - \dots - I_{2N_{2T}N_{2W}} j\omega M_{2N_{2T}N_{2W},1ij} + \end{aligned} \quad (9)$$

and

$$\begin{aligned} V_{2mn} = & I_{111} j\omega M_{111,2mn} - I_{112} j\omega M_{112,2mn} - \dots - I_{1N_{1W}} j\omega M_{11N_{1W},2mn} - \dots - \\ & I_{111} j\omega M_{111,2mn} - \dots - I_{1ij} j\omega M_{1ij,2mn} - \dots - I_{1N_{1W}} j\omega M_{11N_{1W},2mn} - \dots - \\ & I_{1N_{1T}1} j\omega M_{11N_{1T}1,2mn} - I_{1N_{1T}2} j\omega M_{11N_{1T}2,2mn} - \dots - I_{1N_{1T}N_{1W}} j\omega M_{11N_{1T}N_{1W},2mn} + \\ & I_{211} j\omega M_{211,2mn} + I_{212} j\omega M_{212,2mn} + \dots + I_{21N_{2W}} j\omega M_{21N_{2W},2mn} + \dots + \\ & I_{2m1} j\omega M_{2m1,2mn} + \dots + I_{2mn} (R_2 + j\omega L_2) + \dots + I_{2mN_{2W}} j\omega M_{2mN_{2W},2mn} + \dots + \\ & I_{2N_{2T}1} j\omega M_{2N_{2T}1,2mn} + I_{2N_{2T}2} j\omega M_{2N_{2T}2,2mn} + \dots + I_{2N_{2T}N_{2W}} j\omega M_{2N_{2T}N_{2W},2mn} \end{aligned} \quad (10)$$

so

$$V = V_{1ij} + V_{2mn}, \quad (11)$$

where R_1 and R_2 are the resistances for the subconductors in posts 1 and 2, and L_1 and L_2 are the self-inductances of subconductors in post 1 and post 2.

Combining the impedance terms for the same subconductor currents from equations (9) and (10) generates a single impedance coefficient for each subconductor current. By choosing various pairs of subconductors—one from post 1 and one from post 2—a system of equations can be constructed. Unlike the previous case with a single post, a total voltage drop equal to V is not the only boundary condition to the problem. To force a solution for the subconductor currents which insures the total current in post 1 is the same as in post 2, one of the equations in the system must specify that the difference between the sum of the subconductor currents in post 1 and the sum of the subconductor currents in post 2 is zero:

$$\sum_{i=1}^{N_{1r}} \sum_{j=1}^{N_{1w}} I_{ij} - \sum_{m=1}^{N_{2r}} \sum_{n=1}^{N_{2w}} I_{mn} = 0. \quad (12)$$

If the total number of subconductors in the system is given as $N = N_1 + N_2$, then a system of equations containing $N - 1$ voltage drop equations (each using a unique pair of subconductors) and the current boundary condition will determine the unique solution for the subconductor currents.

As in the single-post problem, this system of equations can again be expressed in matrix form. The first N_2 rows express the drop across post 1, subconductor, and post 2, subconductor_{mn} where $m = 1, 2, \dots, N_{2r}$ and $n = 1, 2, \dots, N_{2w}$. Next the drop across post 1, subconductor₁₂ and each of the subconductors in post 2 is used to generate as many as the next N_2 rows. In this manner the first $N - 1$ rows of the matrix are generated. The N th row contains equation (12) to enforce the subconductor current boundary condition. Equation (13) shows the matrix equation for the two-post problem.

$$\begin{bmatrix} V \\ V \\ \vdots \\ V \\ 0 \end{bmatrix} = \begin{bmatrix} R_1 + j\omega(L_1 - M_{111,211}) & j\omega(M_{112,111} - M_{112,211}) & \dots & R_2 + j\omega(L_2 + M_{211,111}) \\ R_1 + j\omega(L_1 - M_{111,212}) & j\omega(M_{112,111} - M_{112,212}) & \dots & j\omega(M_{211,212} - M_{211,111}) \\ \vdots & \vdots & \ddots & \vdots \\ j\omega(M_{212,211} - M_{212,111}) & \dots & j\omega(M_{2N_{2r}N_{2w},211} - M_{2N_{2r}N_{2w},111}) \\ R_2 + j\omega(L_2 - M_{212,111}) & \dots & j\omega(M_{2N_{2r}N_{2w},212} - M_{2N_{2r}N_{2w},111}) \\ \vdots & \vdots & \ddots & \vdots \\ -1 & & & -1 \end{bmatrix} \begin{bmatrix} I_{111} \\ I_{112} \\ \vdots \\ I_{211} \\ I_{212} \\ \vdots \\ I_{2N_{2r}N_{2w}} \end{bmatrix} \quad (13)$$

LU Decomposition is again an advantageous method for inverting the matrix to find the subconductor currents. Once these currents have been determined, a method similar to the single-post problem can be used to determine the impedance of each post.

Substituting the subconductor currents into equations (10) and (11) will yield the voltage drop across chosen subconductors in post 1 and post 2. Since the voltage drop across any subconductor in the post is the same as the voltage drop across the entire post, finding the voltage across one subconductor in each post supplies V_1 across post 1 and V_2

across post 2, where $V = V_1 + V_2$. Next, the total current in each post can be found in the same manner as for the single post:

$$I_1 = \sum_{i=1}^{N_{1r}} \sum_{j=1}^{N_{1w}} I_{ij}, \quad (14)$$

and

$$I_2 = \sum_{m=1}^{N_{2r}} \sum_{n=1}^{N_{2w}} I_{mn}. \quad (15)$$

Since the voltage and current across each of the posts is now known, the impedance for each member of the coupled pair can be found:

$$\frac{V_1}{I_1} = Z_1 = R_{post 1} + j \omega L_{post 1}, \quad (16)$$

and

$$\frac{V_2}{I_2} = Z_2 = R_{post 2} + j \omega L_{post 2}. \quad (17)$$

These impedances are the effective result of the resistance and self-inductance of each post as well as the mutual inductance between posts.

Comparing the impedance results for the two-post solution with the self-impedance found for a single post allows one to quantify the effective difference, at a particular frequency, that the mutual inductance has. Furthermore, graphing the currents for the subconductors allows one to observe how the mutual coupling between the posts, in conjunction with the skin effect, alters their current densities. This task will be undertaken in a later section.

VERIFICATION OF THE IMPEDANCE OF A SINGLE POST

Attempting to measure the impedance of a single conductor is difficult. The fixturing necessary to mount a device under test (DUT) generally contributes some impedance of its own to the measurement. Coupling, in the form of capacitances and mutual inductances between the DUT and the fixturing, is usually difficult to quantify. Consequently, it is often a formidable task to extract the self-impedance of the conductor from the measured data. For these reasons a different approach was taken toward verifying the post impedance.

Well-known formulas exist for computing the frequency-dependent impedance of a round wire. If such a piece of wire is compared to a square post with the same cross-sectional area, similar impedances can be expected at each frequency.

Since both conductors have the same cross-sectional area, their resistance will be the same at dc and should remain similar until the skin effect is well developed. As frequency is increased and the current crowds toward the conductor surface, it will distribute itself equally around the circumference of the wire. However, because the corners of the square post are the farthest points from the center of the conductor, the current in the post will tend to be disproportionately concentrated at the corners. For this reason one would expect to see the resistance of the post increase more quickly than that of the wire.

As the current crowds toward the surface of a conductor, the mean distance between current “elements” increases. With

this increase in mean distance comes a decrease in magnetic flux inside the conductor. As the magnetic flux decreases, the self-inductance of the conductor will also decrease. The same phenomenon responsible for increasing the conductor’s resistivity serves to decrease its self-inductance. If the inductance is separated into two parts—internal inductance and external inductance—a qualitative prediction can be developed for the inductance of the wire versus the post.

The external inductance is only related to the magnetic flux present outside of the conductor. Because this flux is independent of the changing current density inside the conductor, it is also independent of frequency. Flux is determined by the magnetic field distribution. As soon as one moves a short distance from the surface of the post, the field lines begin to assume the same circular orientation as is present around the wire. Consequently, the external inductance of the wire and post will be ostensibly the same and constant over frequency.

The internal inductance, however, is strongly dependent on the internal current distribution. Because the corners of the post are geometrically farther from the interior of the post than the circumference of the wire is from the interior of the wire, the internal inductance of the post will be slightly lower than the internal inductance of the wire. As the frequency increases, this tendency will become increasingly noticeable. Eventually, the frequency will be high enough that the current is so crowded into a thin skin around the perimeter of the conductor, that the internal inductance is virtually zero. As the frequency is increased from this point, the self-inductance of the conductors will remain nearly constant while maintaining a difference attributable to the slight difference in their external inductances.

To test the algorithm and verify these expectations, a piece of 20 AWG copper wire (diameter = 0.032 inch) was compared to a square post with the same cross-sectional area (length of side = 0.0283 inch). Resistance and self-inductance values were computed for a 1-inch length from 1 kHz to 100 MHz.

A three-part calculation was performed to find the impedance of the wire. First, the frequency-dependent resistance of a wire has been shown by Ramo and Whinnery⁴ to be

$$R = \frac{\ell R_s}{\sqrt{2} \pi r} \left[\frac{\text{Ber } q \text{Bei}' q - \text{Bei } q \text{Ber}' q}{(\text{Ber}' q)^2 + (\text{Bei}' q)^2} \right], \quad (18)$$

where

$$R_s = \sqrt{\frac{\pi f \mu}{\sigma}}, \quad q = \sqrt{2 \pi f \mu \sigma} r,$$

and r is the radius of the wire, ℓ is the length of the wire, f is the frequency of interest, σ is the conductivity of copper, and μ is the permeability of copper (the same as air).

Second, Ramo and Whinnery⁴ show the internal inductance of the wire at f to be

$$L_i = \frac{\ell R_s}{2\sqrt{2}\pi^2 f r} \left[\frac{\text{Ber } q \text{ Ber}' q + \text{Bei } q \text{ Bei}' q}{(\text{Ber}' q)^2 + (\text{Bei}' q)^2} \right] \quad (19)$$

Both equations (18) and (19) are in terms of the Ber and Bei Bessel functions where

$$\text{Ber } x + j \text{ Bei } x = J_0(j^{-1/2} x),$$

and Ber' and Bei' are their derivatives.

The third part of the calculation was to find the constant value for the external inductance of the wire. Grover² gives the equation for the self-inductance of nonmagnetic round wire at dc as

$$L = 0.2\ell \left[\ln \frac{2\ell}{r} - \frac{3}{4} \right] \mu H, \quad (20)$$

where all dimensions are in meters. At dc the internal inductance for a round wire is 50 nH/m or 1.27 nH/inch. Subtracting this value from equation (20) yields the external inductance for the wire. Adding the external inductance value to the result from equation (19) furnishes the self-inductance for the wire sample at the chosen frequency.

To compute the impedance of the post, a C program called Post_L was written. Given T , W , ℓ , N_r , N_w , and f , Post_L computes the frequency-dependent impedance of a post using the previously described method. As with any finite approximation method, the greater the number of subconductors in the model, the better the approximation. For this study, Post_L was written and executed on an MS-DOS-based machine. Memory limitations allowed the square post to be divided into an array of subconductors no larger than 14 by 14. It will be seen that further subdivision is necessary to maintain model accuracy at high frequencies.

Table 1 shows the impedance values for the 20 AWG wire and 0.0283-inch-square post.

As expected the resistance and self-inductance values are nearly identical below 50 kHz. This observation is anticipated because below 50 kHz, the skin effect has not yet developed significantly. Consequently, the resistances should be the same while a minor difference in self-inductance is found due to the difference in cross-sectional geometry. In the range from 50 kHz to 1 MHz the resistance of the post rises above that for the wire. Across this same frequency range, the self-inductance of the post decreases slightly faster than the wire. Both results were predicted.

The graphs in Figures 3 and 4 illustrate the resistance and self-inductance data for the wire and square post. Also included are data for a rectangular post with half the thick-

ness (0.01415 inch) and twice the width (0.0566 inch) of the square post. This rectangular post possesses the same cross-sectional area as the wire and square post. The data for the rectangular post are consistent with expectations. Both the resistance and self-inductance should be slightly lower than the square post. In the graphs the subscripts mean the following: w = wire, s = square post, and r = rectangular post.

Table 1

Frequency	Wire Resistance (mΩ)	Wire Self-Inductance (nH)	Post Resistance (mΩ)	Post Self-Inductance (nH)
1 kHz	0.846	20.694	0.848	20.715
2 kHz	0.846	20.694	0.848	20.715
5 kHz	0.847	20.694	0.848	20.715
10 kHz	0.849	20.693	0.850	20.713
20 kHz	0.856	20.687	0.858	20.707
50 kHz	0.905	20.650	0.912	20.666
100 kHz	1.050	20.545	1.069	20.548
200 kHz	1.383	20.319	1.421	20.301
500 kHz	2.067	20.002	2.114	19.966
1 MHz	2.823	19.836	2.839	19.796
2 MHz	3.895	19.716	3.772	19.677
5 MHz	6.028	19.609	5.184	19.582
10 MHz	8.433	19.555	6.078	19.546
20 MHz	11.835	19.517	6.581	19.530
50 MHz	18.587	19.483	6.799	19.524
100 MHz	26.197	19.466	6.836	19.523

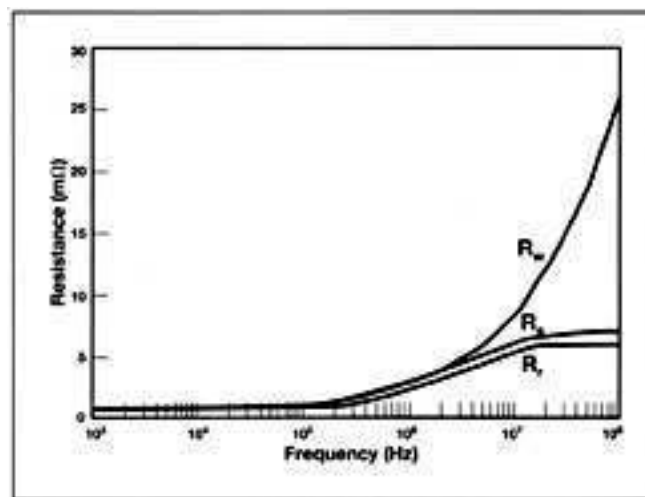


Figure 3. Graph of resistance versus frequency for 20 AWG wire, 0.0283-inch-square post, and 0.0142 x 0.0566-inch-rectangular post.

Above 1 MHz, the graphs show a disturbing trend in the impedance data, particularly the resistance. The resistance calculated for both posts drops off sharply from the well-

known \sqrt{f} dependence displayed by the wire. Likewise, below 1 MHz the self-inductance of the square post decreases faster than the wire. At 10 MHz the self-inductances for the two are about equal. At about 100 MHz the self-inductance of the wire has dropped below that of the post. It would have been expected that the post would maintain a lower inductance than the wire through and beyond the point that the skin effect becomes completely developed.

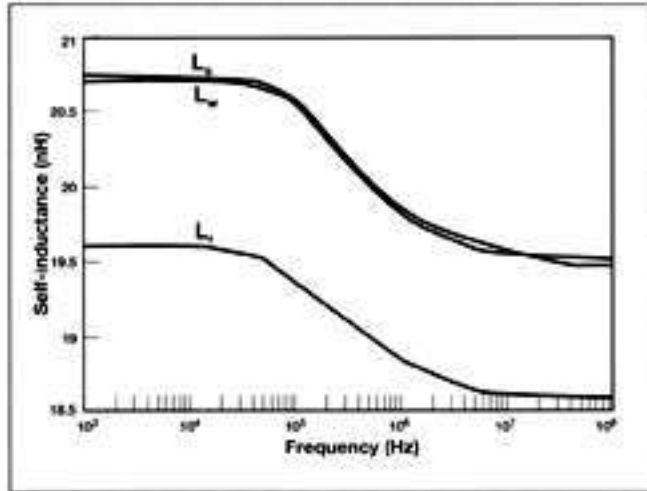


Figure 4. Graph of self-inductance versus frequency for 20 AWG wire, 0.0283-inch-square post, and 0.0142 x 0.0566-inch-rectangular post.

The explanation for this behavior can be traced to the precision of the model. With the square post divided into 14 subconductors in each dimension, each subconductor was a post about 0.0020-inch square. At 1 MHz, the skin depth in copper was calculated to be 0.0026 inch. At this frequency and below, there is more than one subconductor spanning the skin depth. However, as the frequency increases beyond this point, the skin depth soon becomes more shallow than the dimensions of one subconductor. This condition forces the model to represent current as flowing deeper in the conductor than is actually true. Consequently, the 14 by 14 subconductor model becomes a poor approximation at higher frequencies.

These inaccuracies can be alleviated by using more subconductors in the model. For instance, at 100 MHz the skin depth in copper is 0.00026 inch, and a conductor 0.0283 - inch square with one subconductor spanning the skin depth would need a 109 by 109 array of subconductors. Computations of this magnitude can only be handled by large main-frame computers. Therefore, it can be seen that the single-post algorithm performs quite well, but constructing accurate high-frequency models requires extensive computational power.

A surface plot of the current density in the square post at 500 kHz is shown in Figure 5. It is readily seen how the current crowds toward the perimeter of the conductor, particu-

larly at the corners. This graph was made by representing each subconductor's current at its position in the cross section of the square post.

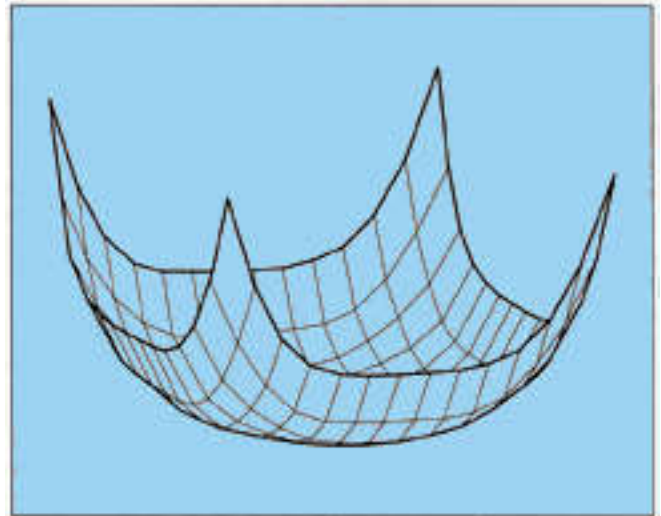


Figure 5. Surface plot of current density in 0.0283-inch-square post.

VERIFICATION OF THE IMPEDANCE OF TWO POSTS EXPERIENCING MAGNETIC COUPLING

Rather than attempting to measure the impedance of the two-post structure shown in Figure 2, a comparison was made with a known reliable calculation method—the finite element method. Finite element modeling has become an accurate and accepted practice for numerically solving the differential equations governing electromagnetic behavior. The method attempts to approximate the geometry of interest with a mesh of triangles. To solve the problem, a system of equations is constructed defining the appropriate differential equation's behavior at the boundaries of each of the triangles in the mesh. Solving the matrix from this system yields the solution to the problem.

To test the two-post impedance algorithm, the following problem was analyzed. Two 0.025-inch-square posts, each 0.5-inch long, were spaced at an 0.050-inch centerline distance. The post material was assumed to be copper. The currents in the posts were identical but flowing in opposite directions. The effective impedances of the posts (including mutual inductances) were computed over the frequency range from 1 kHz to 1 MHz. This frequency range was chosen because of the model inaccuracy problems experienced in the single-post computation.

Ansoft Corporation's Maxwell™ package was used for the finite element modeling. A mesh containing more than 3000 triangles was generated for the geometry. Maxwell's frequency-dependent magnetic solver Eddy™ was used to compute the frequency-dependent resistance and inductance

of the two-post structure. Maxwell is a two-dimensional field solver; it assumes that the length of the geometry is infinite and supplies answers per unit length. To obtain the actual resistance and inductance for the 0.5-inch posts, Ansoft's answers must be multiplied by the post length.

To implement the two-post algorithm, a program called 2 CONDUCTOR MUTUAL was written for an 80386-based machine. Because of the memory limitations experienced with the single-post solution, the program was written and executed using MATLAB™ by The Math Works Inc. MATLAB runs in protected mode on 386-class computers, allowing the user to circumvent DOS-imposed memory barriers. Consequently, each of the two posts could be represented by a 14 by 14 matrix of subconductors in 2CondMut.

Table 2 displays the data collected using Ansoft and 2CondMut at each frequency, while Figures 6 and 7 display graphs of the same values:

Table 2

Frequency	Ansoft Resistance (mΩ)	Ansoft Inductance (nH)	2CondMut Resistance (mΩ)	2CondMut Inductance (nH)
1 kHz	1.0859	7.4867	1.0861	7.2402
2 kHz	1.0859	7.4867	1.0862	7.2401
5 kHz	1.0871	7.4860	1.0870	7.2394
10 kHz	1.0897	7.4829	1.0897	7.2368
20 kHz	1.1024	7.4714	1.1005	7.2267
50 kHz	1.1760	7.4028	1.1696	7.1642
100 kHz	1.3780	7.2377	1.3581	7.0115
300 kHz	1.8326	6.9329	1.7890	6.7261
500 kHz	2.8283	6.4884	2.7221	6.3022
1 MHz	3.9192	6.2484	3.6967	6.0759

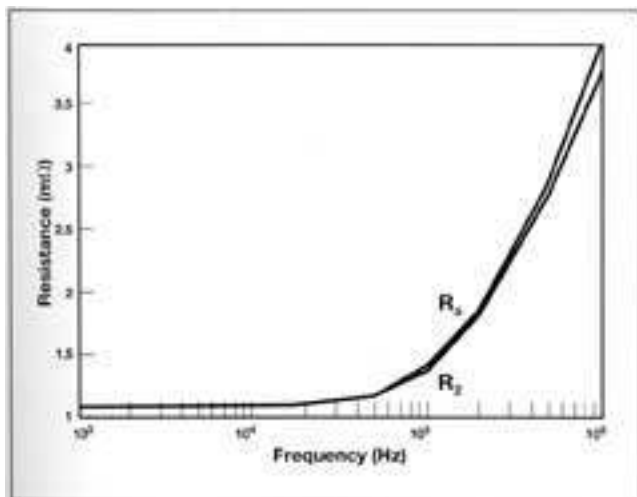


Figure 6. Graph of resistance versus frequency for the two-post problem as solved with Ansoft and 2CondMut.

This table indicates excellent agreement between Ansoft and 2CondMut. Differences between resistance values ranged from virtually zero below 10 kHz to 6% at 1 MHz. Inductance values, on the other hand, showed a consistent difference of 2.8% to 3.4%. It is suspected that much of the difference in the inductance values can be attributed to Ansoft's characteristic of assuming infinite lengths. Such an approach does not account for end effects, i.e., the decrease in inductance per unit length exhibited by the portions of the conductors near the ends of the posts. Therefore, it is likely that the Ansoft results are slightly inflated.

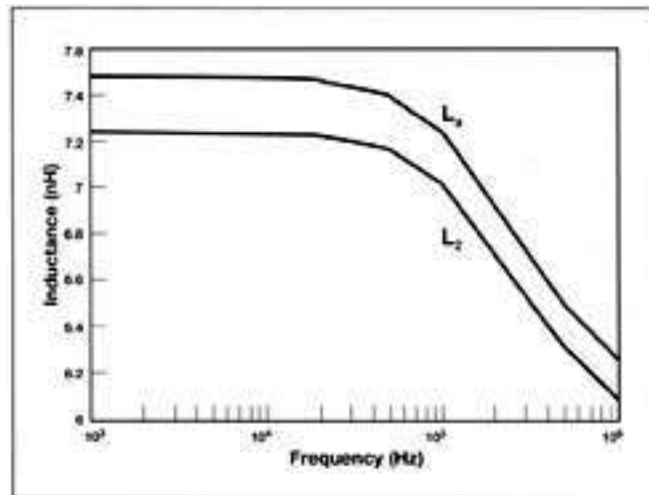


Figure 7. Graph of inductance versus frequency for the two-post problem as solved with Ansoft and 2CondMut.

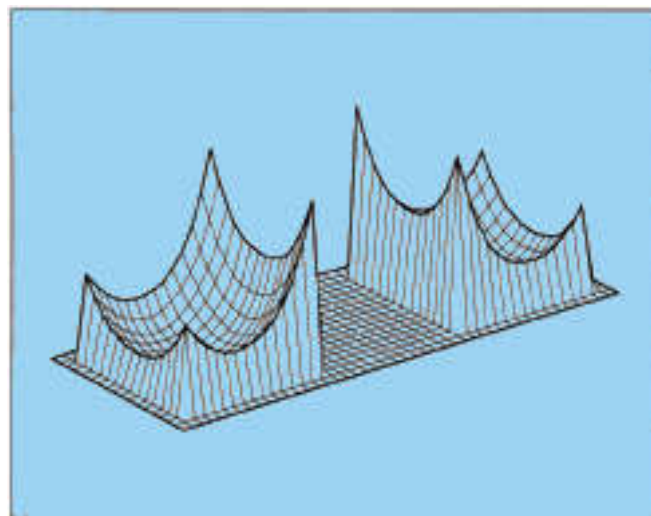


Figure 8. Current density in 0.025-inch-square posts on 0.050-inch centers at 500 kHz.

Typical current densities of the two posts are graphed in Figure 8. This plot is based on computations at a frequency of 500 kHz. The current density in each post is highest at the

inside edges. This distribution is a result of the strong negative mutual inductance occurring between the posts. If the currents had been in the same direction, the greatest density would have been located at the outer edges. The figure also illustrates the influence of the skin effect—the current concentrates at the post perimeter, particularly at the corners. Clearly, the observed current density is dictated by the combined influence of the mutual inductance between the posts and the skin effect.

CONCLUSION

Two methods have been described for computing the impedance of conducting posts with rectangular cross sections. The first method, intended for computing the resistance and self-inductance of an isolated post, divides the post into subconductors and constructs a matrix equation based on the voltage drop across the post. The second method analyzes the combined impedance of two posts experiencing mutual coupling. This later technique is not only based on a uniform voltage drop across each post, but must also satisfy the requirement of providing identical current magnitudes in each post.

Comparison of the results of these techniques with other benchmarks revealed accurate correlation. The expectations for marginally higher resistance and slightly lower self-inductance were realized for the single post when compared to a round wire of identical cross-sectional area. Computational accuracy was found to be sensitive to the number of subconductors spanning the skin depth. Because this condition affects the frequency range over which a given size model can be accurately used, a reduced frequency range was applied to the two-post problem. Comparison between Ansoft's finite element solution for this problem and the previously described algorithm revealed agreement within a few percent across the frequency range. It was postulated that some of the observed discrepancy may be due to Ansoft assuming infinite lengths for the conductors and not accounting for end effects.

Because of the generality of these calculations, it is interesting to note that no constraint exists barring the application of these techniques to conductors of arbitrary cross sections. Furthermore, the technique applied to the coupled post prob-

lem could be expanded to assess the impedance of systems containing more than two conductors. However, the computational horsepower needed to tackle such problems with higher frequencies or multiple conductors dictates the use of work stations or mainframe computers.

REFERENCES

1. B.E. Keiser, *Principles of Electromagnetic Compatibility* (Artech House Inc., Dedham, Massachusetts, 1979), p. 102, equation (5.4).
2. F.W. Grover, *Inductance Calculations, Working Formulas, and Tables* (Dover Publications, New York, 1946).
3. W.N. Press, B.P. Flannery, S.A. Teukolsky, and W.T. Vetterling, *Numerical Recipes in C, The Art of Scientific Computing* (Cambridge University Press, New York, 1989), pp. 39-45.
4. S. Ramo, J.R. Whinnery, and T. Van Duzer, *Fields and Waves in Communication Electronics* (John Wiley & Sons, New York, 1984), pp. 178-182.
5. P. Lorrain and D.R. Corson, *Electromagnetic Fields and Waves* (W. H. Freeman and Company, San Francisco, 1970).
6. W.T. Weeks, L.L. Wu, M.F. McAllister, and A. Singh, "Resistive and Inductive Skin Effect in Rectangular Conductors," *IBM J. Res. Dev.* 23(6), 652-660(1979).

Alexander W. Barr is a Development Engineer in the Technology Group at AMP Incorporated in Harrisburg, Pennsylvania.

Mr. Barr received a B.A. in physics from Franklin & Marshall College in Lancaster, Pennsylvania, and is currently pursuing an M.S. in electrical engineering from the Pennsylvania State University. Since joining AMP in 1984, he has been responsible for analyzing the electrical performance of connectors, contacts, and related devices through computer modeling, time-domain reflectometry, and microwave measurements.